Daple coordinates organ-wide and cell-intrinsic polarity to pattern inner-ear hair bundles

Kimberly Siletti[a,b], Basile Tarchini[c,1,2], and A. J. Hudspeth[a,b,1,2]

[a]Howard Hughes Medical Institute, The Rockefeller University, New York, NY 10065; [b]Laboratory of Sensory Neuroscience, The Rockefeller University, New York, NY 10065; and [c]The Jackson Laboratory, Bar Harbor, ME 04609

Contributed by A. J. Hudspeth, November 13, 2017 (sent for review September 19, 2017; reviewed by Michael Deans and Matthew W. Kelley)

The establishment of planar polarization by mammalian cells necessitates the integration of diverse signaling pathways. In the inner ear, at least two systems regulate the planar polarity of sensory hair bundles. The core planar cell polarity (PCP) proteins coordinate the orientations of hair cells across the epithelial plane. The cell-intrinsic patterning of hair bundles is implemented independently by the G protein complex classically known for orienting the mitotic spindle. Although the primary cilium also participates in each of these pathways, its role and the integration of the two systems are poorly understood. We show that Dishevelled-associating protein with a high frequency of leucine residues (Daple) interacts with PCP and cell-intrinsic signals. Regulated by the cell-intrinsic pathway, Daple is required to maintain the polarized distribution of the core PCP protein Dishevelled and to position the primary cilium at the abneural edge of the apical surface. Our results suggest that the primary cilium or an associated structure influences the domain of cell-intrinsic signals that shape the hair bundle. Daple is therefore essential to orient and pattern sensory hair bundles.

auditory system | cochlea | hair cell | planar cell polarity | primary cilium

The systematic orientation of cells within an epithelium is termed planar cell polarity (PCP). A striking example of PCP involves the hair cell, the sensory receptor cell of the inner ear. On the apical surface of each mature hair cell stands a hair bundle that comprises a few tens to a few hundreds of rigid, actin-filled stereocilia arranged in a staircase pattern. The hair cell's primary cilium, the kinocilium, stands at the tall edge of the staircase. The hair bundle's morphological asymmetry signals its functional polarization: Deflection of the bundle toward its tall edge opens channels at the tips of the stereocilia, depolarizes the cell, and excites the associated nerve fibers (1). Stimulation in the opposite direction elicits inhibition, and orthogonal deflection is without effect. Because each hair bundle is responsive along a specific axis, hearing and balance require that this axis of sensitivity correspond with that of mechanical stimulation. Acoustic stimulation, in particular, evokes mechanical vibrations along an axis that runs radially from the center of the cochlea toward its periphery, that is, between the neural and abneural edges of the organ of Corti (Fig. 1*A*).

During the development of the inner ear, individual hair bundles must deploy their polarized hair bundles so as to achieve directional mechanosensitivity. Moreover, all of the hair cells in each sensory organ must be organized to align their axes of sensitivity with the direction of stimulation. These two requirements are accomplished during development by signaling systems that are, in large part, independent. The orientation of hair cells within the sensory epithelium of each receptor organ follows a "compass" instantiated by the core PCP system. In *Drosophila*, an epithelial cell's planar orientation is specified by the asymmetrical distribution of six core PCP proteins: Frizzled, Dishevelled, Diego, van Gogh, Prickle, and Flamingo (2). Mammals possess homologs of each of these proteins (3). Because each hair bundle in a core PCP mutant maintains its normal shape but is misoriented in the epithelial plane (4, 5), PCP signals coordinate the organ-wide orientations of neighboring hair cells but not the cell-intrinsic polarity of individual hair cells.

The cell-intrinsic patterning of each cell is determined instead by an apical molecular "blueprint" comprising proteins that are classically known for orienting the mitotic spindle during asymmetrical cell division (6–8). The alpha subunit of inhibitory heterotrimeric G protein (Gαi), G protein signaling modulator 2 (Gpsm2), and mammalian Inscuteable (Insc) colocalize beneath the flat apical membrane between the tall edge of the hair bundle and the abneural edge of each hair cell (Fig. 1*B*); partitioning defective 3 homolog (Pard3) occurs along the abneural edge of the cell. Atypical protein kinase C (aPKC) forms a complementary domain on the opposite side of the cell. Disruption of this network disrupts the position of the kinocilium on the apical surface, resulting in a split or otherwise misshapen hair bundle (6–9).

A key issue in cochlear development is the mechanism by which the asymmetry of individual hair bundles is reconciled with the PCP of the cochlear sensory epithelium. How, in other words, is the cellular blueprint aligned with the global compass? Although the core PCP system might regulate G protein signals to position the kinocilium and orient the hair bundle, no molecular link between the two systems has been identified. In addition, some evidence suggests a more complex sequence of events. Mispositioning of the kinocilium or basal body in a *Mkks*$^{-/-}$, *Bbs8*$^{-/-}$, or *Ift88*$^{-/-}$ hair cell expands the distribution of Gαi, implying that kinocilia influence the cell-intrinsic signaling pathway (6, 8, 10). Moreover, the kinocilium undergoes two

Significance

Each hair cell of our auditory and vestibular systems transduces stimuli into electrical signals through its mechanosensitive hair bundle. Because the bundle is responsive along only a single axis, its orientation is crucial. Two systems determine hair-bundle polarity: planar cell polarity proteins, which establish axes along which hair cells are oriented, and the proteins Gαi and LGN. Investigating how these two systems are coordinated so that each hair bundle is appropriately aligned, we identified Daple. In mutants lacking Daple, hair bundles are misoriented and misshapen, a phenotype suggestive of both organ-wide and cell-intrinsic defects. Our study indicates how Daple interacts with proteins of the two systems and proposes a model for its role in determining hair-bundle polarity.

Author contributions: K.S., B.T., and A.J.H. designed research; K.S. and B.T. performed research; K.S. and B.T. analyzed data; and K.S., B.T., and A.J.H. wrote the paper.

Reviewers: M.D., University of Utah; and M.W.K., National Institutes of Health.

The authors declare no conflict of interest.

[1]B.T. and A.J.H. contributed equally to this work.

[2]To whom correspondence may be addressed. Email: hudspaj@rockefeller.edu or basile.tarchini@jax.org.

This article contains supporting information online at www.pnas.org/lookup/suppl/doi:10.1073/pnas.1716522115/-/DCSupplemental.

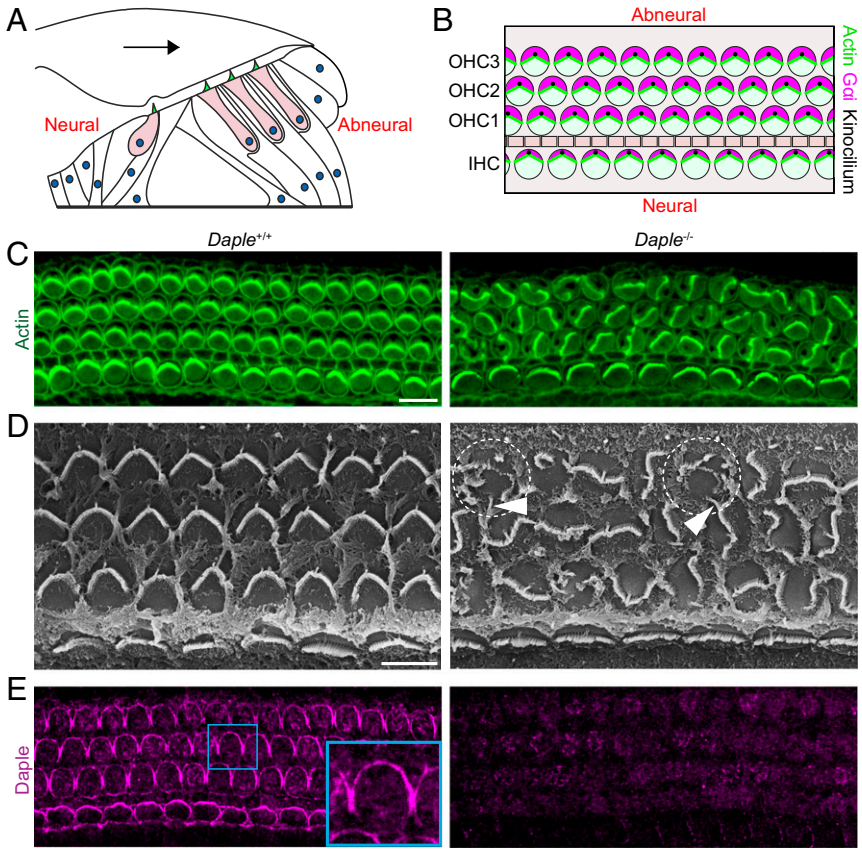

Fig. 1. Daple in cochlear hair-bundle development. (*A*) Schematic diagram of the cochlear sensory epithelium, the organ of Corti, depicts one row of inner hair cells and three rows of outer hair cells (pink) surmounted by the gelatinous tectorial membrane. Up-and-down vibration of the basilar membrane causes mechanical stimulation along the neural-to-abneural axis (arrow). (*B*) Schematic representation of the surface of the organ of Corti portrays the single row of inner hair cells (IHC) and the three rows of outer hair cells (OHC). Each hair bundle (green) forms an arrowhead pointed toward the abneural edge of the sensory epithelium. A kinocilium (black dot) stands at the apex of each bundle, and the domain of Gαi expression (pink) extends from the hair bundle to the abneural edge of the cell. (*C*) Phalloidin labeling (green) reveals hair bundles in a postnatal day (P) 0 wild-type cochlea (*Left*) and a *Daple*$^{-/-}$ littermate (*Right*). Although wild-type bundles orient toward the abneural edge of the cochlea, *Daple*$^{-/-}$ hair bundles are misshapen and do not orient uniformly. (Scale bar: *C* and *E*, 10 μm.) (*D*) Scanning electron micrographs portray hair bundles from P2 wild-type and *Daple*$^{-/-}$ animals. Most of the mutant bundles are misoriented and deformed, and some are fragmented (dashed circles; kinocilia at arrowheads). (Scale bar: 5 μm.) (*E*, *Left* and *Inset*) Immunohistochemistry reveals Daple (magenta) at the abneural boundaries of wild-type P0 hair cells. (*E*, *Right*) This junctional enrichment is not visible in *Daple*$^{-/-}$ littermates.

movements during hair cell maturation: A shift toward the abneural cortex in immature hair cells is followed by a neural relocalization coincident with early hair bundle development (7). Although the enrichment of Gαi at the abneural surface roughly coincides in orientation with the initial shift of the kinocilium, the two are not perfectly correlated (7). Instead, their alignment is refined as the kinocilium relocalizes neurally.

To elucidate the sequence of events that pattern the hair bundle, we conducted a yeast two-hybrid screen to seek proteins that interact with Gαi, a central component of the cell-intrinsic signaling system.

Results

The Loss of Daple Causes Severe Hair-Bundle Defects. Using full-length Gαi3 as bait, we screened a cDNA library derived from 600 inner ears of mice aged 2 to 6 d (Table S1). As expected, the screen identified the Gαi regulator Gpsm2, also termed Leu-Gly-Asn repeat-enriched protein (LGN). Immunohistochemical localization of several other candidates revealed expression in the nucleus, membrane-bounded organelles, or cellular cortex (Fig. S1). Prominent among the products of the screen was the coiled-coil domain-containing protein 88c (Ccdc88c), also termed Dishevelled-associating protein with a high frequency of leucine residues (Daple). A Dishevelled-binding protein that inhibits canonical Wnt signaling in *Xenopus*, Daple also directs cell migration through noncanonical Wnt signaling (11, 12). Moreover, Daple is a guanine nucleotide exchange factor that can bind and activate Gαi3 downstream of Wnt (13). The interactions of Daple with both Dishevelled and Gαi3 have been demonstrated by coimmunoprecipitation (13–15). Because Daple can regulate both Gαi and the core PCP protein Dishevelled, we sought to characterize the protein's role in hair-bundle development.

Adult animals of the *Ccdc88c*$^{tm1(KOMP)Mbp}$ strain, subsequently referred to as *Daple*$^{-/-}$ mutants, resembled their heterozygous littermates. Their cochleae, each containing one row of inner hair cells and three rows of outer hair cells (Fig. 1*B*), were grossly normal at birth (Fig. S2*A*). Although the absence of Daple did not affect the organization of these four rows, *Daple*$^{-/-}$ mice displayed striking defects in their hair bundles. The staircase of stereocilia was both misoriented and grossly misshapen (Fig. 1*C*). Because the *Ccdc88c*$^{tm1(KOMP)Mbp}$ strain contained a floxed neomycin-resistance cassette (Fig. S2*B*), we confirmed that *Ccdc88c*$^{tm1b(KOMP)Mbp}$ with no neomycin-resistance cassette also exhibited hair-bundle defects (Fig. 1*D*). We verified the genomic deletion by sequencing and RT-PCR (Fig. S2 *B* and *C*).

To further investigate whether the genetic deletion eliminated Daple function, we conducted immunohistochemistry with two antibodies that target parts of the protein outside the genetic

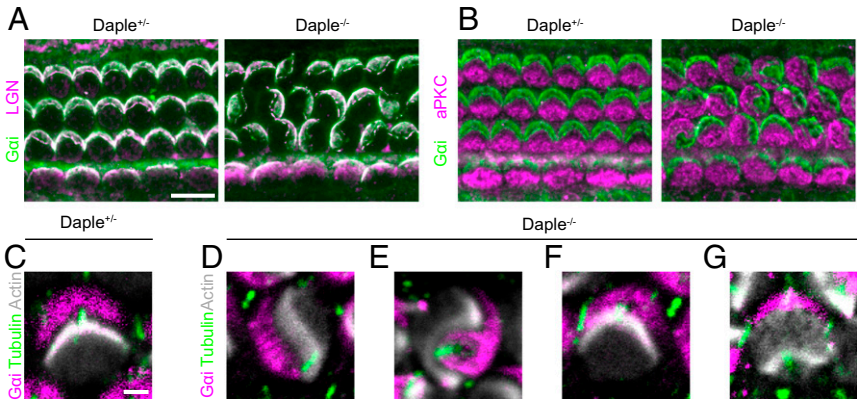

Fig. 2. Cell-intrinsic blueprint for planar polarity in postnatal *Daple*$^{-/-}$ hair cells. (*A*) Immunohistochemistry demonstrates that Gαi (green) and LGN (magenta) colocalize at the apical surfaces of hair cells in postnatal day 1 *Daple*$^{+/-}$ (*Left*) and *Daple*$^{-/-}$ (*Right*) littermates. (Scale bar: *A* and *B*, 10 μm.) (*B*) Gαi (green) and aPKC (magenta) form complementary domains in *Daple*$^{+/-}$ (*Left*) and *Daple*$^{-/-}$ (*Right*) littermates. (*C*–*G*) Immunohistochemistry reveals the kinocilium (acetylated tubulin, green) and the domain of Gαi (magenta) in individual hair cells. Phalloidin (gray) labels actin in the hair bundle. (Scale bar: *C*–*G*, 2 μm.) (*C*) In a control hair cell, the kinocilium is centered within the domain of Gαi. (*D*–*F*) As in *C*, the hair bundles in *Daple*$^{-/-}$ hair cells border the edges of the Gαi domains. (*D*) Kinocilium lies at one end of the Gαi domain in a hair cell with an S-shaped bundle. (*E*) Kinocilium occurs near the center of a hair cell with a C-shaped bundle. (*F*) Kinocilium is centered within the domain of Gαi expression in a hair cell that resembles the control. (*G*) In a *Daple*$^{-/-}$ hair cell, the bundle is fragmented when the kinocilium opposes the crescent of Gαi expression.

deletion. Both antibodies revealed Daple at the abneural intercellular junctions of cochlear cells, an enrichment not visible in *Daple*$^{-/-}$ mice (Fig. 1*E* and Fig. S3). Both Dishevelled and Gαi localized on the abneural side of cochlear hair cells (16–18), suggesting that Daple is positioned to interact both with core PCP components and with cell-intrinsic signals.

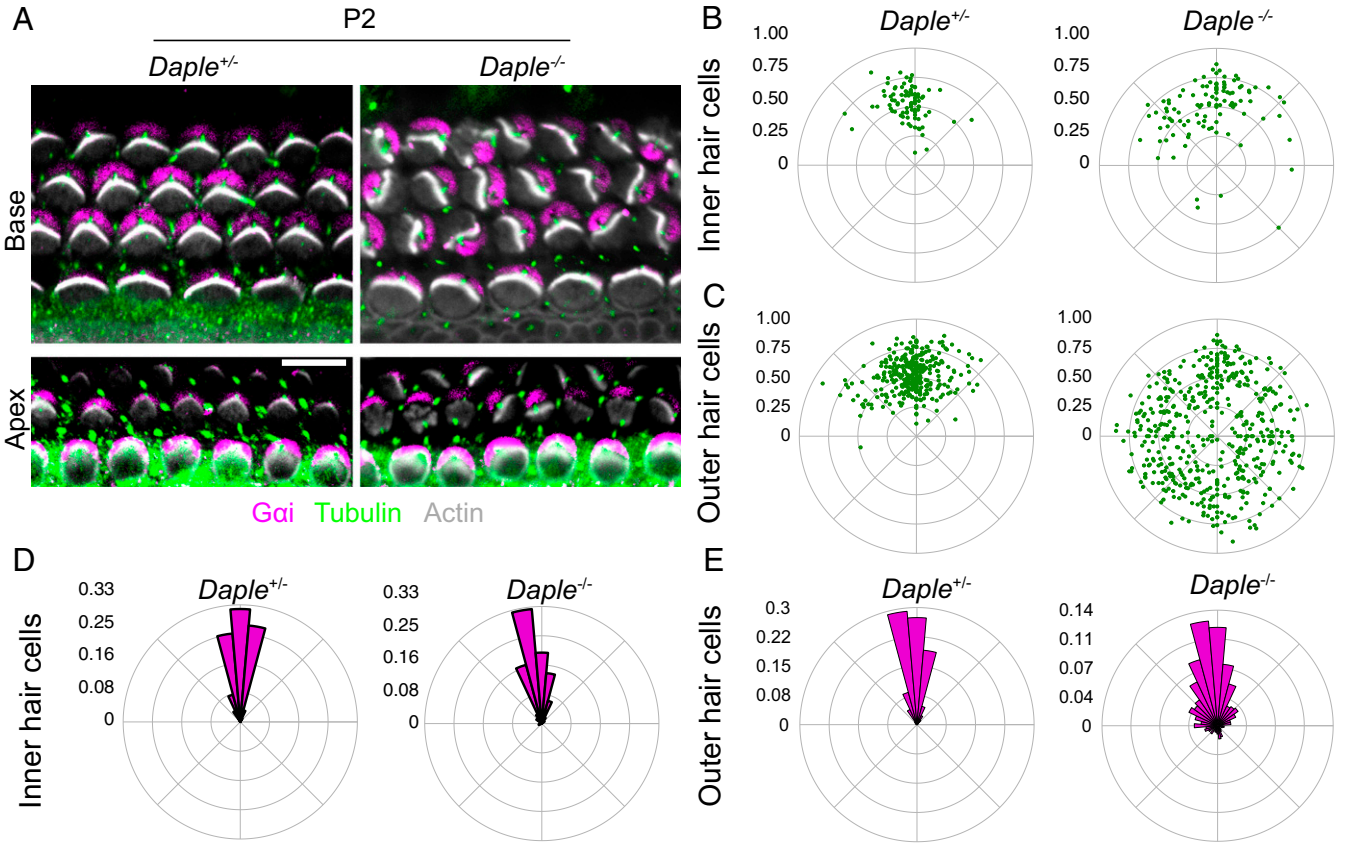

Fig. 3. Hair cell misorientation and kinociliary defects in the absence of Daple. (*A*) Near the base (*Top*) and apex (*Bottom*) of a postnatal day (P) 2 cochlea, immunolabeling of acetylated tubulin reveals the positions of the kinocilia (green) in *Daple*$^{+/-}$ (*Left*) and *Daple*$^{-/-}$ (*Right*) littermates. Phalloidin (gray) and antibodies against Gαi (magenta) label the apical surface of each hair cell. (Scale bar: 10 μm.) (*B*) For each of 88 *Daple*$^{+/-}$ and 105 *Daple*$^{-/-}$ inner hair cells, the position of the kinocilium (green) is plotted with respect to the apical surface. Whereas the kinocilia localize midway between the cell centers and the abneural edges of *Daple*$^{+/-}$ hair cells (*Left*), kinocilia are widely distributed and occur even in the neural halves of the cells in the absence of Daple (*Right*). (*C*) Position of the kinocilium (green) is plotted with respect to the apical surface for each of 350 wild-type and 495 *Daple*$^{-/-}$ outer hair cells. Whereas kinocilia localize in the abneural half of a *Daple*$^{+/-}$ hair cell (*Left*), they adorn the entire apical surfaces in the absence of Daple (*Right*). (*D*) For inner hair cells, the angles from the cellular centers to the middles of the Gαi3 domains are summarized in a polar histogram. The Gαi3 domains are only mildly misoriented in *Daple*$^{-/-}$ inner hair cells (*Right*) compared with heterozygous littermates (*Left*). (*E*) For P2 outer hair cells, the angles of the centers of the Gαi3 domains are summarized in a polar histogram. Although Gαi is biased toward the abneural edge in both *Daple*$^{+/-}$ (*Left*) and *Daple*$^{-/-}$ (*Right*) littermates, the latter exhibit orientation defects. Whereas in control cochleae the most abneural 10° bin captures nearly 30% of the hair cells, in *Daple*$^{-/-}$ cochleae the most abneural bin includes fewer than 14%.

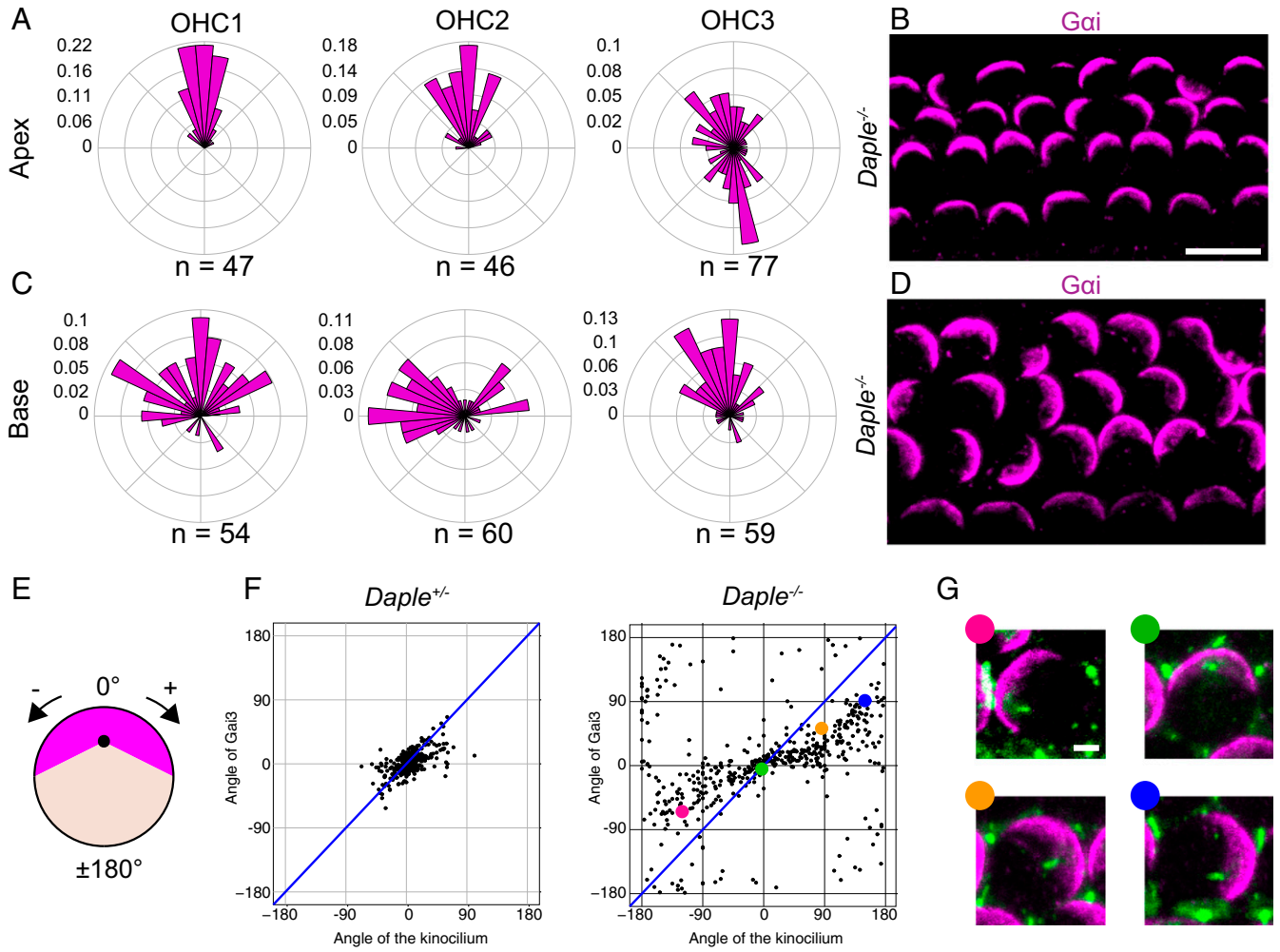

Fig. 4. Characterization of orientation defects in *Daple*$^{-/-}$ hair cells. (*A*) For each row of outer hair cells (OHC) near the apex of the cochlea, the angles from the cell centers to the middles of the Gαi3 domains are summarized in a polar histogram. *Daple*$^{-/-}$ mutants exhibit the most severe orientation defects in the third row of OHC. A single neural bin captures nearly 10% of hair cells in the third row. (*B*) Near the apex of a cochlea, maximal-intensity projections reveal the domain of Gαi (magenta) in each hair cell. The hair cells of *Daple*$^{-/-}$ animals exhibit misoriented Gαi3 domains, particularly in the two most abneural rows of OHC. (Scale bar: *B* and *D*, 10 μm.) (*C*) For each row of OHC near the base of the cochlea, the angles from the cell centers to the middles of the Gαi3 domains are summarized in a polar histogram. *Daple*$^{-/-}$ mutants exhibit the most severe orientation defects in the first two rows of OHC. (*D*) Near the base of a cochlea, maximal-intensity projections reveal the domain of Gαi in each hair cell. The hair cells of *Daple*$^{-/-}$ animals exhibit misoriented domains of Gαi3 expression, particularly in the first two rows of OHC. (*E*) In a schematic diagram, an angle of 0° denotes the abneural edge in a wild-type hair cell. Gαi expression (pink) and the kinocilium (black dot) are depicted. (*F*) Angle of the kinocilium with respect to each hair cell's center is plotted against the angle of the middle of the Gαi3 domain in the same cell. Although the data from heterozygous littermates cluster about the blue identity line (*Left*), the data from *Daple*$^{-/-}$ mice reveal a more complex relationship between the two angles (*Right*). (G) *Daple*$^{-/-}$ hair bundles are displayed from different regions of the graph in *F*, in which each bundle can be identified by its associated color (pink, green, orange, and blue). (Scale bar, 2 μm.)

Coupling of Gαi and the Kinocilium Shapes the Hair Bundle. Although postnatal *Daple*$^{-/-}$ hair bundles were severely misshapen, the apical enrichment of cell-intrinsic signals did not appear diminished. LGN colocalized with Gαi3, and aPKC formed a complementary domain (Fig. 2 *A* and *B*). Instead, postnatal *Daple*$^{-/-}$ hair cells exhibited a variety of hair-bundle shapes characterized by the relationship between Gαi3 and the kinocilium. In wild-type cells, the kinocilia were always centered within the Gαi3 domains (Fig. 2*C*). In some *Daple*$^{-/-}$ cells, the kinocilia lay near the corners of the Gαi3 domains, correlating with S-shaped bundles (Fig. 2*D*). In other cells, the kinocilia more closely aligned with the Gαi3 domain but were shifted toward the centers of the apical surfaces. Gαi3 spread to encompass the kinocilia, and the cells exhibited C-shaped bundles (Fig. 2*E*). In a third subset of cells, the kinocilia adopted approximately normal positions and the hair bundles resembled those of wild-type animals (Fig. 2*F*).

In a final subset of hair cells, Gαi3 was entirely uncoupled from the kinocilia (Fig. 2*G*). In each of these cells, the kinocilium localized near the neural edge, whereas Gαi3 formed an abneural crescent. Although the stereocilia formed misshapen but cohesive bundles that bordered Gαi3 (Fig. 2 *C*–*F*) in most hair cells, the stereocilia of these cells grew in a disperse pattern, extending from the border of the Gαi3 domain toward the kinocilium and encircling it. These hair bundles may correspond to the fragmented bundles visualized by scanning electron microscopy (Fig. 1*D*). This result provides evidence that coupling of the kinocilium and Gαi is crucial to maintain the coherent structure of the hair bundle.

Postnatal *Daple*$^{-/-}$ Hair Cells Exhibit Planar-Polarity Defects. We quantified cell-intrinsic defects by immunolabeling the kinocilia

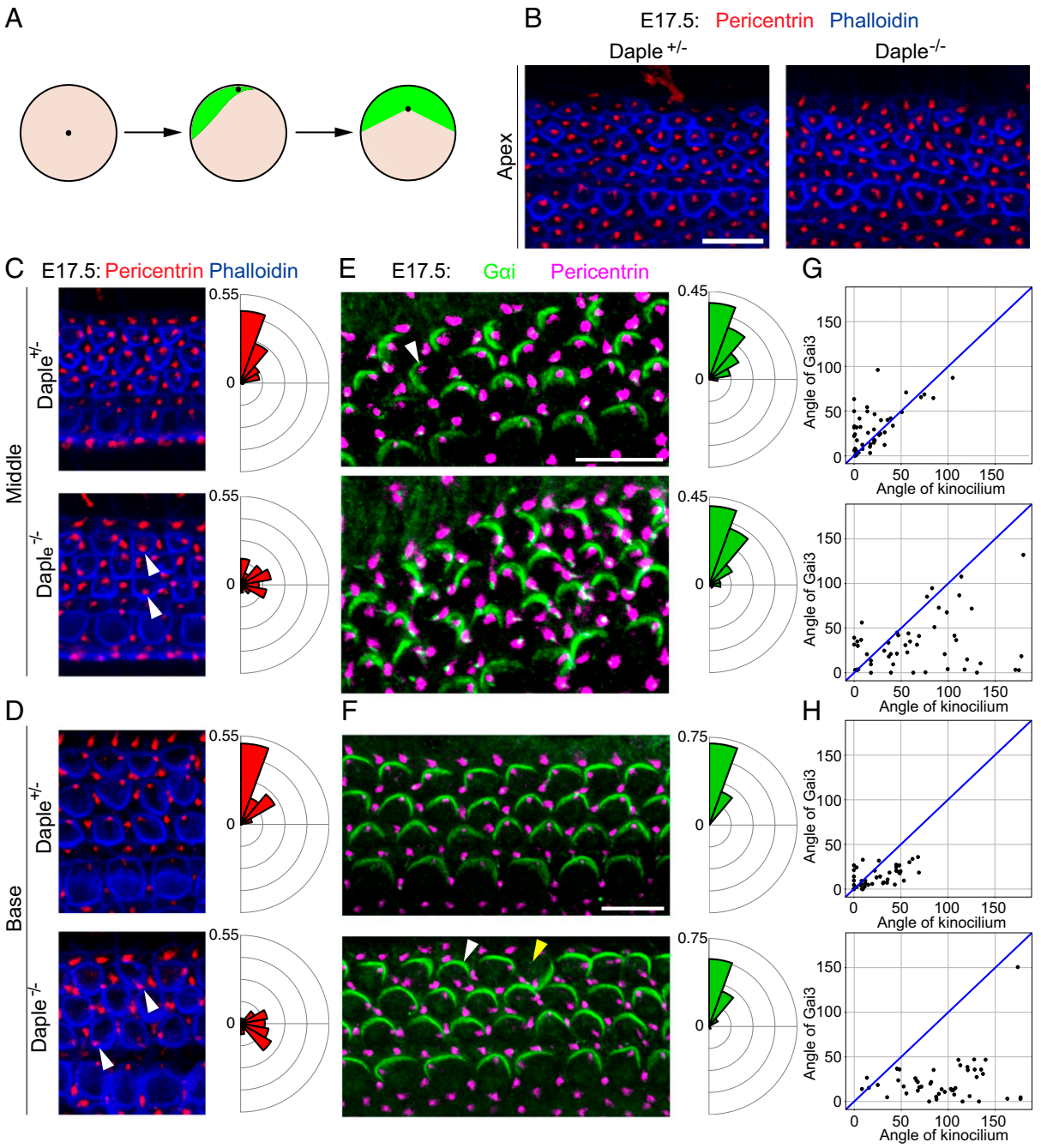

Fig. 5. Misalignment of Gαi and kinocilia in E17.5 *Daple*$^{-/-}$ hair cells. (*A*) Schematic diagram depicts the sequence of hair cell maturation. (*Left*) Kinocilium (black dot) lies at the center of an immature hair cell. (*Center*) Enrichment of Gαi (green) coincides with the initial shift of the kinocilium toward the cell's abneural edge. (*Right*) Domain of Gαi is then refined as the kinocilium relocates toward the center of the cell. (*B*) At the cochlear apex, immunolabeling of pericentrin (red) and phalloidin (blue) staining reveals the positions of the kinocilia relative to the intercellular junctions of *Daple*$^{+/-}$ (*Left*) and *Daple*$^{-/-}$ (*Right*) littermates. Kinocilia lie near the centers of hair cells of both genotypes. (Scale bar: *B*–*D*, 10 μm.) (*C*) In middle cochlear turns, the hair cells of a heterozygous animal exhibit kinocilia primarily at their abneural edges, whereas many *Daple*$^{-/-}$ kinocilia occur at the neural edges (arrowheads). On the right side of each panel, the angular positions of the kinocilia with respect to the centers of the cells are summarized in a radial histogram. The absolute value of each angle is shown. (*D*) Basal hair cells of heterozygous animals exhibit kinocilia primarily at their abneural edges, whereas many *Daple*$^{-/-}$ kinocilia occur at the neural edges (arrowheads). The radial histograms on the right side of each panel emphasize that the proportion of kinocilia in the neural halves of the hair cells increases toward the cochlear base. (*E*) Immunolabeling of middle cochlear turns for Gαi (green) and pericentrin (magenta) discloses that the Gαi3 domains are comparably oriented in *Daple*$^{+/-}$ (*Top*) and *Daple*$^{-/-}$ (*Bottom*) hair cells. Although the Gαi3 domains are misoriented in some *Daple*$^{+/-}$ hair cells, the kinocilia occur at the abneural edges of the same cells (arrowhead). On the right side of each panel, the angular positions of the Gαi3 domains with respect to the centers of the cells are summarized in a radial histogram. The absolute values of the angles are shown. (Scale bar: 10 μm.) (*F*) Immunolabeling of cochlear bases as in *E* shows that the distribution of Gαi is similar in heterozygous (*Top*) and *Daple*$^{-/-}$ (*Bottom*) hair cells. One of 100 *Daple*$^{-/-}$ hair cells is inverted (yellow arrowhead). In many *Daple*$^{-/-}$ hair cells, the kinocilia lie near the edges of the Gαi domains; in a few cells, the kinocilia are opposite the crescents of Gαi (white arrowhead). (Scale bar: 10 μm.) (*G*) Absolute values of the angles of the kinocilia and Gαi3 domains are plotted as in Fig. 4*F* for middle cochlear turns. Although the data from heterozygous littermates cluster near or above the blue identity line (*Top*), the data from *Daple*$^{-/-}$ mice are largely distributed below the identity line (*Bottom*). (*H*) For cochlear bases, the angles of the kinocilia and Gαi3 domains are plotted as in *G*. Although the data from heterozygous littermates cluster about the blue identity line (*Top*), the data from *Daple*$^{-/-}$ mice are distributed below the identity line (*Bottom*).

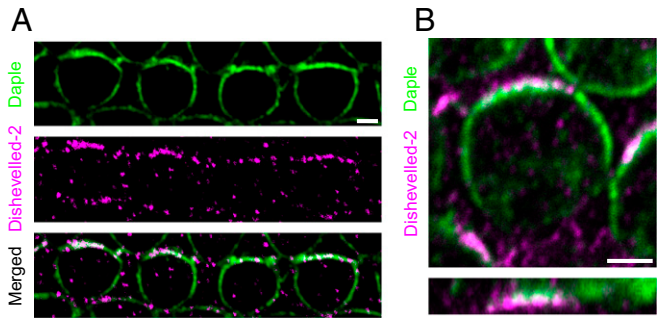

Fig. 6. Localization of Daple and Dishevelled in hair cells. (*A*) Immunohistochemistry demonstrates that Daple (green) and Dishevelled2 (magenta) colocalize in postnatal day 0 hair cells. (Scale bar: 2 μm.) (*B*, *Top*) Projection of a Z-stack in the *x*–*y* plane demonstrates that Daple (green) and Dishevelled2 (magenta) colocalize in cochlear explants. (*B*, *Bottom*) Projection of the same stack in the *x*–*z* plane demonstrates that Daple overlaps with Dishevelled and extends apically. (Scale bar: 2 μm.)

(Fig. S4). Unlike the kinocilia of heterozygous littermates, which occurred near the abneural edges of hair bundles, the kinocilia of *Daple*$^{-/-}$ hair cells were distributed across the apical surfaces (Fig. 3 *A*–*C*). Because disruption of the core PCP pathway affects the angular positions of the kinocilia but not their distances from the cellular boundaries, the randomized distribution of kinocilia in outer hair cells signaled a defect in cell-intrinsic polarity.

To quantify the defects associated with organ-wide polarity, we used the localization of Gαi3 to denote the orientations of hair cells within the cochlear sensory epithelium (Fig. S4). For individual *Daple*$^{+/-}$ and *Daple*$^{-/-}$ hair cells, we plotted the angles of the Gαi3 domains with respect to the centers of the apical surfaces. The domain of Gαi3 was misoriented in both inner and outer hair cells (Fig. 3 *D* and *E*), with more significant defects in the latter ($P < 0.01$ and $P < 0.001$, respectively). However, the localization of Gαi3 was still biased toward the abneural edges of *Daple*$^{-/-}$ hair cells.

We further characterized the contributions of organ-wide and cell-intrinsic signals to the *Daple*$^{-/-}$ phenotype by comparing orientation defects among the three rows of outer hair cells. In *Looptail* mutants lacking Vangl2, the third or outermost row of outer hair cells is the most affected, whereas the first row is the least disturbed (4, 19, 20). This trend was apparent near the apices of *Daple*$^{-/-}$ cochleae, where a greater number of hair cells

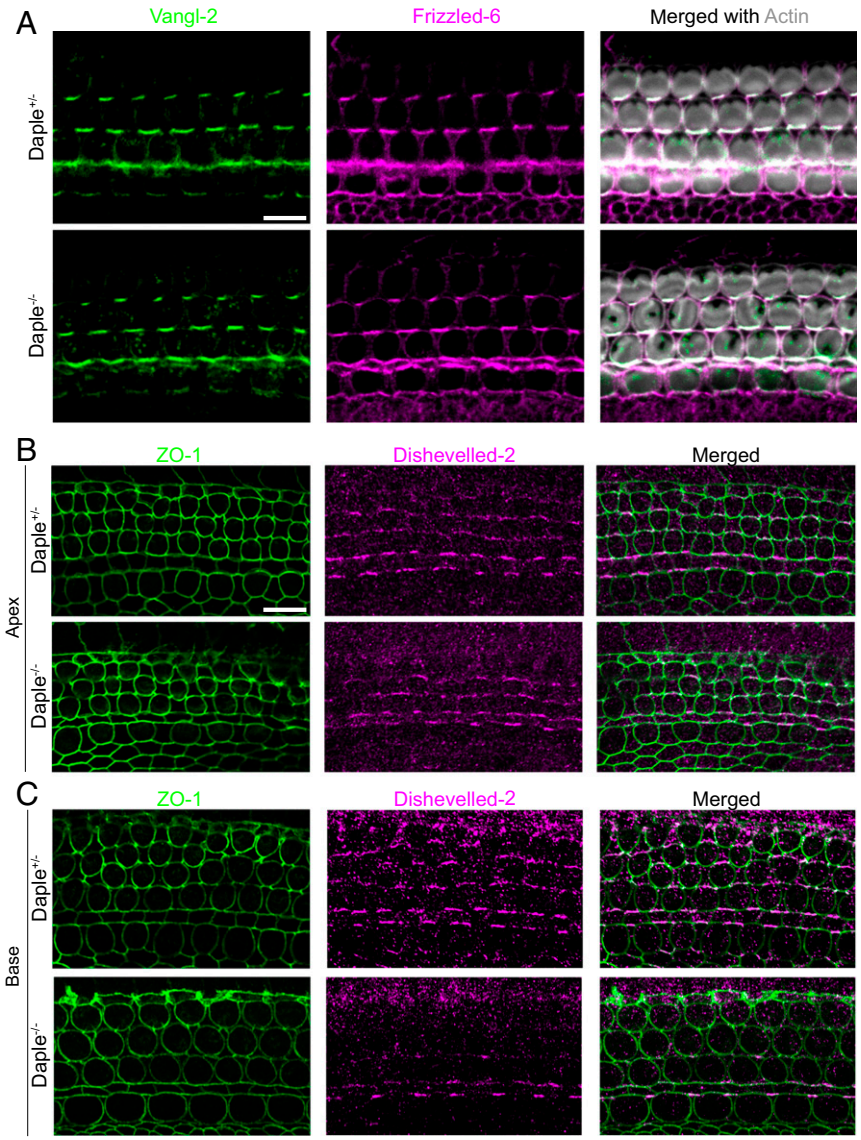

Fig. 7. Localization of core PCP signals in the absence of Daple. (*A*) Immunohistochemistry shows that Vangl2 (green) and Frizzled6 (magenta) occur at the neural junctions between hair cells and supporting cells in both heterozygotes (*Top*) and *Daple*$^{-/-}$ postnatal day (P) 2 littermates (*Bottom*). Phalloidin labeling (gray) emphasizes that both proteins are asymmetrically distributed despite the severe bundle defects apparent in *Daple*$^{-/-}$ mice (merged, *Right* column). (Scale bar: 10 μm.) (*B*) ZO-1 (green), which marks tight junctions, and Dishevelled (magenta) are immunolabeled near the apex of *Daple*$^{+/-}$ (*Top*) and *Daple*$^{-/-}$ (*Bottom*) P0 cochleae. Dishevelled occurs at the abneural edges of *Daple*$^{-/-}$ hair cells. (Scale bar: 10 μm.) (*C*) ZO-1 (green) and Dishevelled (magenta) are immunolabeled near the base in *Daple*$^{+/-}$ (*Top*) and *Daple*$^{-/-}$ (*Bottom*) P0 littermates. Although Dishevelled localizes asymmetrically in wild-type cochleae, the protein is absent from the abneural edges of *Daple*$^{-/-}$ hair cells. (Scale bar: 10 μm.)

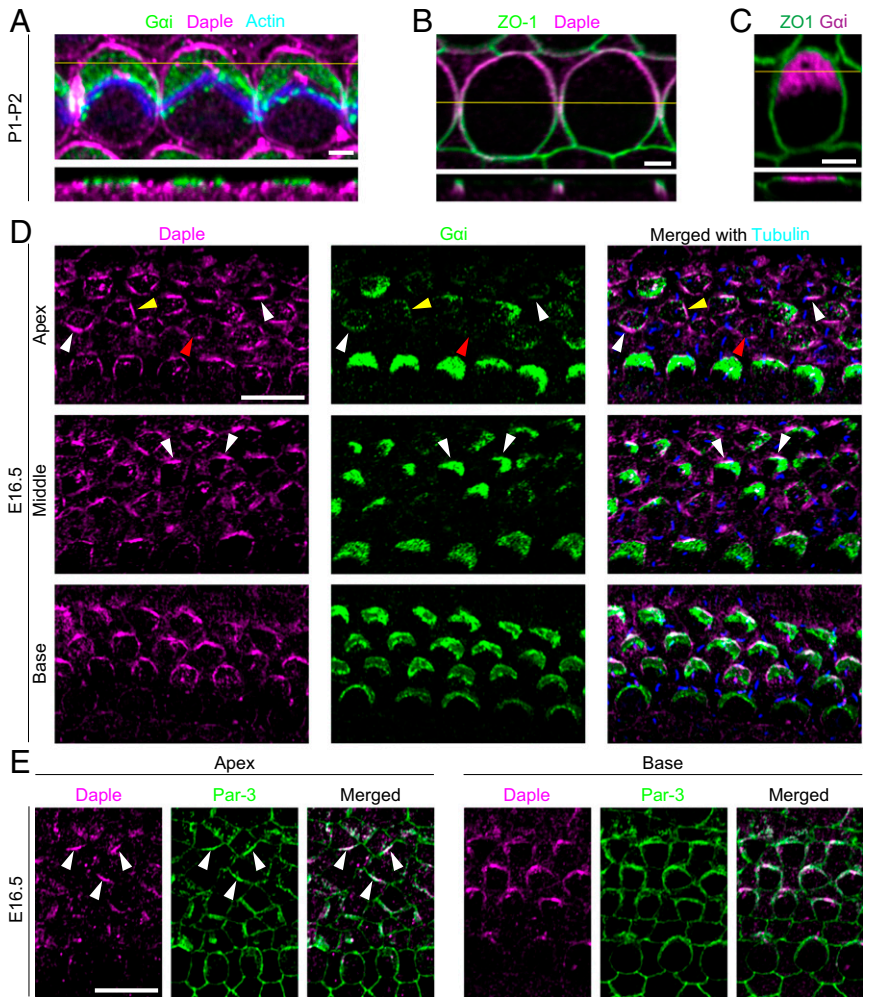

Fig. 8. Localization of Daple and cell-intrinsic planar-polarity proteins during hair cell development. (*A*, *Top*) Projection of a Z-stack in the *x*–*y* plane demonstrates the immunohistochemical localizations of Gαi (green) and Daple (magenta) at the apical surface of a postnatal day (P) 2 outer hair cell. Phalloidin (blue) labels actin in the hair bundle. (*A*, *Bottom*) Projection of the same stack in the *x*–*z* plane at the position of the yellow line demonstrates that Gαi localizes more apically than Daple, which occurs at the level of the intercellular junctions. (Scale bar: 2 μm.) (*B*, *Top*) Near the base of a P1 cochlea, immunolabeling of ZO-1 (green) and Daple (magenta) confirms that Daple abuts these junctions. (*B*, *Bottom*) Projection of the stack in the *x*–*z* plane at the position of the yellow line suggests that Daple colocalizes with ZO-1 and might extend more basolaterally. (Scale bar: 2 μm.) (*C*, *Top*) Near the apex of a P1 cochlea, immunolabeling of ZO-1 (green) and Gαi (magenta) establishes that Gαi is excluded from the intercellular junctions. (*C*, *Bottom*) Projection of the stack in the *x*–*z* plane at the position of the yellow line establishes that Gαi is restricted to the apical surface of the hair cell. (Scale bar: 2 μm.) (*D*, *Top*) In an E16.5 cochlea immunolabeled for Daple (magenta), Gαi (green), and acetylated tubulin (blue), many immature hair cells near the cochlear apex express Daple and Gαi. The distributions of the two proteins are similar (yellow arrowheads). In some hair cells, neither protein is asymmetrically distributed (red arrowheads); in other cells, both proteins occur at the neural edge (white arrowheads). (*D*, *Middle*) Daple and Gαi are confined to the abneural halves of some hair cells (white arrowheads). (*D*, *Bottom*) Near the base of the cochlea, Daple and Gαi are closely correlated in orientation, and their domains expand in surface area. (Scale bar: 10 μm.) (*E*, *Left*) Near the apex of an E16.5 cochlea immunolabeled for Daple (magenta) and Pard3 (green), the two proteins are enriched at the neural edges of several immature outer hair cells (white arrowheads). (*E*, *Right*) Near the base, Daple and Pard3 are distributed abneurally in more mature hair cells. Pard3 is also junctional in supporting cells with no obvious planar polarization. (Scale bar: 10 μm.)

were reversed in the third row of outer hair cells than in the other two rows (Fig. 4 *A* and *B*). In contrast, near the bases of *Daple*$^{-/-}$ cochleae, the third row exhibited milder orientation defects than did the other two rows (Fig. 4 *C* and *D*). Increased severity of misorientation in the first row of outer hair cells, rather than the third row, occurs after exposure to the G protein inhibitor pertussis toxin (6, 7). The apices of *Daple*$^{-/-}$ cochleae thus resembled those of core PCP mutants, whereas the bases suggested cell-intrinsic defects. The data therefore supported our observation of organ-wide and cell-intrinsic defects in *Daple*$^{-/-}$ hair cells.

Because the kinocilia in *Daple*$^{-/-}$ hair cells were no longer biased in the abneural direction, we wondered to what extent localization of the kinocilia remained correlated with G protein signals. We therefore compared the angle of the Gαi3 domain and the corresponding angular position of the kinocilium with respect to each cell's center. Although the two angles were correlated in both *Daple*$^{-/-}$ mice and heterozygous littermates, the correlation was imperfect in the absence of Daple (Fig. 4 *E*–*G*). When the domain of Gαi3 expression was oriented toward the abneural edge of the hair cell, the kinocilium could be found in either half of that domain. This relationship changed when the domain of Gαi3 shifted away from the abneural edge; when Gαi3 was misoriented, the kinocilium then occurred preferentially in the neural half of the Gαi3 domain.

Daple$^{-/-}$ Kinociliary Defects Precede Gαi3 Mislocalization. To explain this trend, we investigated the developmental progression of the relationship between Gαi3 and the kinocilium (Fig. 5*A*). Hair cell maturation proceeds in a gradient from the cochlear base toward the apex. Although in both *Daple*$^{+/-}$ and *Daple*$^{-/-}$ cochleae at embryonic day (E) 17.5, nearly all kinocilia were located near the centers of hair cells at the apex, we found very few central kinocilia at the base (Fig. 5 *B*–*D*). The initial off-center shift of the kinocilia toward the cellular boundaries therefore occurred in the absence of Daple. Because kinocilia lay near the centers of postnatal *Daple*$^{-/-}$ hair cells (Fig. 3*C*), the second shift of the kinocilium evidently occurred as well. Both movements exhibited directional errors: In 47 of 141 hair cells in the middle turn of an E17.5 *Daple*$^{-/-}$ cochlea, the kinocilia were displaced in the neural direction, whereas only three of 134 kinocilia of a heterozygous littermate showed such a shift (Fig. 5*C*). Near the bases of *Daple*$^{-/-}$ cochleae, 66 of 119 kinocilia were displaced in the neural direction, whereas the kinocilia of heterozygous littermates were uniformly abneural (Fig. 5*D*). Early errors in the initial shift of the kinocilia were therefore augmented by relocalization defects as hair cells matured.

In contrast, the angular distributions of Gαi3 were comparable in E17.5 *Daple*$^{+/-}$ and *Daple*$^{-/-}$ cochleae near both the middle turn and the base (Fig. 5 *E* and *F*; $P > 0.5$ and $P > 0.1$, respectively). In immature hair cells near the middle cochlear turns, Gαi3 domains were not yet precisely oriented in either *Daple*$^{+/-}$ or *Daple*$^{-/-}$ mice (Fig. 5*E*). In more mature hair cells near the cochlear bases, Gαi3 was distributed abneurally in both genotypes (Fig. 5*F*). *Daple*$^{-/-}$ Gαi3 crescents were not yet misshapen as in postnatal cells.

Near the middle turn of a *Daple*$^{+/-}$ cochlea, most kinocilia were aligned with the Gαi3 domains or found closer to the abneural

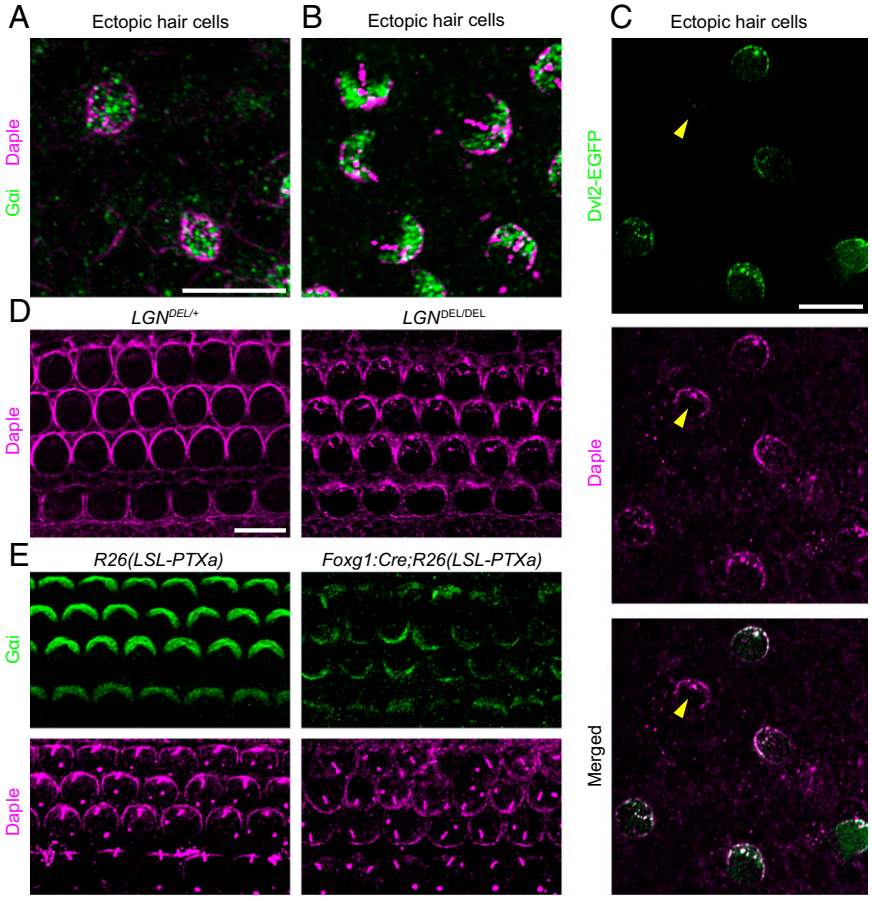

Fig. 9. Cell-intrinsic regulation of Daple and Dishevelled. (*A* and *B*) Daple (magenta) and Gαi (green) are immunolabeled in ectopic hair cells induced by the electroporation of *Atoh1-IRES-EGFP* into cochlear explants. Ectopic hair cells were identified by EGFP expression and actin-positive hair bundles. (*A*) Neither Daple nor Gαi is asymmetrically localized in two hair cells. (Scale bar: *A* and *B*, 10 μm.) (*B*) In another subset of ectopic hair cells, both Daple and Gαi are asymmetrically localized and match perfectly in orientation even though the hair cells are not oriented uniformly. The labeling of the kinocilia is nonspecific. (*C*) Coelectroporation into cochlear explants of plasmids for untagged *Atoh1* and *Dvl2-EGFP* generates ectopic hair cells expressing fluorescently tagged Dishevelled protein. A hair cell-specific *Atoh1* enhancer drives the expression *of Dvl2-EGFP*. Endogenous Daple (magenta) and Dvl2-EGFP (green) colocalize in ectopic hair cells, forming asymmetrical crescents with similar planar orientation. Cells transfected with only *Atoh1* (yellow arrowheads) exhibit an asymmetrical pattern of endogenous Daple (magenta) but no Dvl2-EGFP (green). (Scale bar: 10 μm.) (*D*) Daple is immunolabeled in postnatal day 1 $LGN^{DEL/+}$ (*Left*) and $LGN^{DEL/DEL}$ cochleae (*Right*). Daple is depleted from the abneural junctions of $LGN^{DEL/DEL}$ hair cells and enriched near the bases of the kinocilia. (Scale bar: *D* and *E*, 10 μm.) (*E*) *Foxg1-cre* knock-in animals are crossed with transgenic mice that express Cre-induced pertussis toxin. Control (*Left*) and toxin-expressing (*Right*) E18.5 cochleae are immunolabeled for Gαi (green) and Daple (magenta). Both proteins occur at the abneural edges of control hair cells but are depleted by pertussis toxin. The toxin also inverts the first two rows of outer hair cells as well as the domains of Gαi and Daple. The labeling of the kinocilia is nonspecific.

edges of the hair cells (Fig. 5*G*). Gαi3 and the kinocilia more closely aligned near the base of the cochlea (7) (Fig. 5*H*). In the absence of Daple, the kinocilia were frequently farther from the abneural edges of the hair cells than were the centers of the Gαi3 domains (Fig. 5*G*). This effect was most severe at the base (Fig. 5*H*). As in postnatal mice, some kinocilia lay opposite the crescents of Gαi3. The data imply that although the kinocilium sometimes preceded the Gαi3 domain at the abneural edge of a wild-type hair cell, the abneural distribution of Gαi3 did not rely on similar positioning of the kinocilium.

Daple Interacts with Dishevelled and the Cell-Intrinsic Pathway. To identify potential partners of Daple in the core PCP or cell-intrinsic pathways, we conducted a second yeast two-hybrid screen. Using the carboxyl-terminal half of Daple protein as bait, we isolated 66 candidates, including Gαi3 and Gαi2 (Table S2). Among the most frequently detected candidates were the three Dishevelled proteins. Although Daple extended more apically than Dishevelled2, the two proteins colocalized in cochlear hair cells (Fig. 6 and Fig. S5). We therefore investigated whether Daple is necessary for the localization of PCP proteins. The core PCP components Vangl2 and Frizzled6 were distributed similarly in $Daple^{+/-}$ and $Daple^{-/-}$ cochleae (Fig. 7*A*). With zonula adherens 1 (ZO-1) as a label for cellular boundaries, we found that Dishevelled2 also occurred normally near the cochlear apices of $Daple^{-/-}$ mice (Fig. 7*B*). Near the bases of $Daple^{-/-}$ cochleae, however, Dishevelled2 was absent from the abneural edges of hair cells (Fig. 7*C*). These observations suggest that Daple maintained the localization of Dishevelled as hair cells matured.

Using ZO-1 as a marker for tight junctions, we compared Daple and Gαi3 in postnatal hair cells. Daple overlapped with and extended below the junction, whereas Gαi3 was found above the junction at the apical membrane (Fig. 8 *A*–*C*). Daple and Gαi3 therefore occupied distinct but adjacent subcellular compartments, but their subcellular domains coincided in orientation during embryonic development. As early as E16.5, Daple and Gαi3 were visibly enriched at the apical surfaces of immature hair cells near the apex of the cochlea (Fig. 8*D*). Moreover, the proteins were enriched in similar regions of each cell; in a subset of cells, both proteins occurred at the neural cellular boundaries. Their localizations were refined in more mature hair cells near the base of the cochlea, adopting an abneural distribution (Fig. 8*D*). Furthermore, Daple clearly colocalized with Pard3 in both apical and basal hair cells, confirming that Daple associates with junctional cell-intrinsic signals (Fig. 8*E*). Like Gαi3, Pard3 and Daple colocalized near the neural boundaries of some immature hair cells. Because our yeast two-hybrid assay with Daple revealed two isoforms of Pard3, the immunohistochemical colocalization of Daple and Pard3 likely reflected an authentic biochemical interaction.

Because Daple and other cell-intrinsic polarity signals exhibited similar subcellular asymmetry in each region of the cochlea, we asked whether Daple exhibits cell-intrinsic polarity in solitary hair cells. Electroporation of *Atoh1-IRES-EGFP* plasmids into cochlear explants produced hair cells in the greater epithelial ridge of the cochlea, a region normally devoid of hair cells (21). Although these ectopic hair cells were not aligned consistently along any axis, the subcellular localizations of Daple and Gαi3 remained closely correlated. In a subset of ectopic hair cells, neither protein was asymmetrically distributed (Fig. 9*A*): Daple associated with junctions at the circumference of the cells, whereas Gαi3 expanded across the entire apical surfaces. In most cells, however, both Daple and Gαi3 were asymmetrically distributed with the

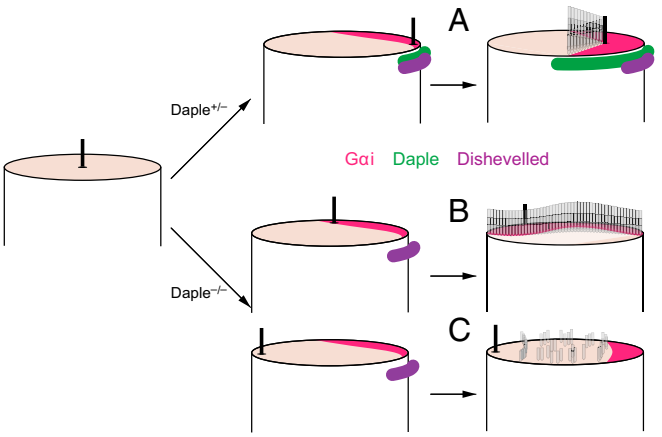

Fig. 10. Daple's role in hair-bundle orientation and development. (*Left*) Kinocilium (black) occurs near the center of immature hair cells in both *Daple*$^{+/-}$ and *Daple*$^{-/-}$ mice. (*A*) As a wild-type hair cell matures, the kinocilium shifts toward the abneural edge. (*Left*) Dishevelled (purple) localizes at the abneural junction of the hair cell, and Gαi (pink) is enriched at the abneural apical surface. Gαi and LGN also promote the enrichment of Daple at the abneural junction. (*Right*) In a mature hair cell, the kinocilium shifts toward the center of the cell. The distributions of Daple and Gαi become closely correlated and also extend toward the center of the cell. The hair bundle develops along the edge of the Gαi domain. (*B*, *Left*) In the absence of Daple, Dishevelled still becomes enriched at the abneural junction of the hair cell; Gαi is enriched at the abneural apical surface. The kinocilium, however, may not complete its abneural shift. (*B*, *Right*) As the hair cell matures, the kinocilium may even shift toward the neural edge of the cell, modulating the domain of Gαi. The hair bundle develops along the edge of the Gαi domain. Dishevelled does not persist at the abneural edge of the hair cell. (*C*, *Left*) In other *Daple*$^{-/-}$ hair cells, the kinocilium does not undergo an initial abneural movement but, instead, shifts neurally. (*C*, *Right*) As the hair cell matures, Gαi forms a crescent opposite the kinocilium. The hair bundle is fragmented across the apical surface between Gαi and the kinocilium. Dishevelled does not persist at the abneural edge of the hair cell.

same orientation (Fig. 9*B*). Daple therefore associated with cell-intrinsic markers in the absence of organ-wide directional cues.

Because the maintenance of Dishevelled in hair cells required Daple, we wondered whether Dishevelled might also exhibit cell-intrinsic polarity in ectopic hair cells. We therefore coelectroporated *Atoh1* and *Dvl2-EGFP* plasmids into cochlear explants. Dvl2-EGFP was enriched asymmetrically and colocalized with Daple in ectopic hair cells (Fig. 9*C*), suggesting that Daple provides a link between G protein signals and Dishevelled.

Because cell-intrinsic signals appeared sufficient to specify the asymmetry of Daple and Dishevelled, we inquired whether G protein signals are necessary for the normal localization of Daple at hair cell junctions. We performed immunohistochemistry in LGN$^{-/-}$ mice. In the absence of LGN, Gαi and Insc were depleted from the apical surface (7). We found that Daple was significantly reduced at abneural junctions and occurred near the bases of kinocilia (Fig. 9*D*). Although anti-Daple sometimes labeled kinocilia in both wild-type and *Daple*$^{-/-}$ tissues (Fig. S3), the label did not accumulate near the bases of kinocilia. Thus, the pattern observed in *LGN*$^{-/-}$ mice likely reflected a change in the distribution of Daple.

Pertussis toxin inactivates G protein signaling in hair cells without disrupting core PCP signals (6, 7, 22). To test the role of Gαi directly, we therefore used a *Foxg1-cre* transgenic mouse (23) to express pertussis toxin (24) throughout the embryonic cochlea. Gαi3 was depleted but detectable at apical hair cell surfaces (Fig. 9*E*). As in the absence of LGN, Daple occurred asymmetrically but was diminished at intercellular junctions. The expression of pertussis toxin inverted the orientations of the first two rows of outer hair cells so that the tall edges of their hair bundles faced neurally (6, 7) (Fig. 9*E*). Daple localization was also inverted in those cells, confirming that Daple is regulated primarily by G protein signals rather than by core PCP proteins.

Discussion

We propose that the Dishevelled-binding protein Daple shapes the cell-intrinsic blueprint of a developing hair cell by coordinating the position of the kinocilium with the crescent of Gαi expression. Our results imply that during embryonic development, LGN and Gαi promote the enrichment of Daple at the abneural junction of each hair cell. Gαi is enriched independent of Daple in a crescent at the abneural surface of each hair cell; this initial pattern is then modulated by the kinocilium or its appendages as the hair cell matures (Fig. 10*A*).

To our knowledge, *Daple*$^{-/-}$ animals are the first mutants to be described in which kinocilia are mislocalized across hair cell surfaces despite the presence of apical G proteins. When kinocilia are mispositioned in the absence of Daple, G protein signals are evidently reoriented and expanded toward the kinocilium as a hair cell matures. Hair cells therefore develop organ-wide and cell-intrinsic polarity defects (Fig. 10*B*). This hypothesis explains the tendency in a postnatal *Daple*$^{-/-}$ hair cell for the kinocilium to occur in the neural half of the Gαi3 domain; the postnatal orientation of the Gαi3 domain represents a compromise between its embryonic abneural distribution and the angular position of the kinocilium. Also consistent with this hypothesis, some postnatal *Daple*$^{-/-}$ hair cells exhibit an abneural crescent of Gαi3 but a neural kinocilium (Fig. 10*C*). These cells likely result from defects in the initial shift of the kinocilium; mislocation in the neural direction precludes the kinocilium from modulating abneural Gαi localization. It is interesting that our yeast two-hybrid screen identified RGS14, a regulator of G protein signaling previously characterized as a centrosomal protein (25, 26).

Daple is also crucial for patterning the hair bundle. Previous studies have suggested that the cell-intrinsic blueprint proteins determine hair-bundle shape (7). We accordingly observe that the edge of the developing hair bundle abuts the domain of Gαi3 in both wild-type cells and most Daple-deficient cells (Fig. 10 *A* and *B*). In the absence of Daple, the staircase pattern of stereocilia is distorted but preserved when the kinocilium occurs near the Gαi domain. In contrast, when Gαi and the kinocilium occur on opposite sides of a hair cell, the hair bundle becomes highly fragmented (Fig. 10*C*). Stunted stereocilia often encircle the kinocilium, suggesting that the kinocilium can also promote stereociliary elongation. Together with the observation that normal positioning of the kinocilium in a *Daple*$^{-/-}$ mutant rescues bundle shape, these results indicate that Gαi3 and the kinocilium cooperate to shape the hair bundle.

Because Gαi occurs abneurally in embryonic *Daple*$^{-/-}$ hair cells, the loss of Daple does not uniformly affect all manifestations of organ-wide orientation but disrupts the association between the crescent of G protein signals and the kinocilium. However, neither Daple nor the Gαi crescent appears to be necessary for the initial movement of the kinocilium away from the center of a hair cell. Even those kinocilia opposite the crescent of Gαi reach the cellular boundaries. An additional pathway might regulate the migration of the kinocilium, with Daple aligning this system with the apical crescent of Gαi and LGN. Daple might activate Gαi directly. Although the two proteins do not colocalize in postnatal hair cells, they might interact at earlier stages of hair cell development or at the boundaries of their subcellular distributions. During asymmetrical divisions of mammalian cells, nuclear mitotic-apparatus protein (NuMA) binds the microtubule motor Dynactin to couple the mitotic spindle to cortical Gαi and LGN (27). In our yeast two-hybrid assay, Daple interacted with Dynactin and other microtubule-associated proteins. Daple might therefore couple microtubules with Gαi, Pard3, or even Dishevelled, which can also regulate mitotic-spindle orientation (28).

The absence of Daple affected outer hair cells more severely than inner hair cells, suggesting that different mechanisms contribute to

PCP and intrinsic polarization in different cell types. Daple also influences the translational and rotational polarity of the cilia in ependymal cells (29). Although Daple is evidently necessary in that context for the accumulation of Frizzled, we find that Frizzled6 expression is unaffected by the absence of Daple in the cochlea; instead, Daple is necessary to maintain the localization of Dishevelled.

Although *Dishevelled* mutants display core PCP defects, the localization of a Dvl2-EGFP fusion construct in BAC transgenic mice differs from that of other core PCP proteins (17). Whereas in Vangl-2 *Looptail* mutants, Frizzled3 fails to localize, Dvl2-EGFP is diminished but still asymmetrically distributed. Furthermore, we found that Dvl2-EGFP localizes with cell-intrinsic signals in ectopic hair cells (Fig. 9*C*). These results imply that Daple provides a conduit through which cell-intrinsic polarity signals affect the distribution of a core PCP factor. Because Daple interacts both with apical Gαi proteins and with junctional Dishevelled, it is well positioned to link these two systems.

Materials and Methods

Experiments were conducted in accordance with the policies of the Institutional Animal Care and Use Committees of The Rockefeller University and The Jackson Laboratory. Use of the coding sequence for *Mus musculus* Gαi3 in a yeast two-hybrid screen identified Daple as a potential interaction partner. Immunohistochemistry was used to demonstrate the location of the Daple protein in cochlear specimens from wild-type and *Daple*$^{-/-}$ [*Ccdc88c*$^{tm1b(KOMP)Mbp}$] mice. Additional details are provided in *Supporting Information*.

ACKNOWLEDGMENTS. We thank The Rockefeller University's Comparative Bioscience Center for animal husbandry and in vitro fertilization services, Stephen Freeman for an immunohistochemistry protocol, and Ksenia Gnedeva and the members of the authors' research groups for comments on the manuscript. We especially thank Adrian Jacobo for providing the program to quantify hair-bundle defects and for many helpful discussions. K.S. was supported by the National Institute on Deafness and Other Communication Disorders (NIDCD) through a Ruth L. Kirschstein National Research Service Award (DC014212). B.T. was supported by NIDCD Grant DC015242 and by The Jackson Laboratory. A.J.H. is an Investigator of the Howard Hughes Medical Institute.

1. Hudspeth AJ (2014) Integrating the active process of hair cells with cochlear function. *Nat Rev Neurosci* 15:600–614.
2. Simons M, Mlodzik M (2008) Planar cell polarity signaling: From fly development to human disease. *Annu Rev Genet* 42:517–540.
3. Ezan J, Montcouquiol M (2013) Revisiting planar cell polarity in the inner ear. *Semin Cell Dev Biol* 24:499–506.
4. Montcouquiol M, et al. (2003) Identification of Vangl2 and Scrb1 as planar polarity genes in mammals. *Nature* 423:173–177.
5. Wang Y, Guo N, Nathans J (2006) The role of Frizzled3 and Frizzled6 in neural tube closure and in the planar polarity of inner-ear sensory hair cells. *J Neurosci* 26: 2147–2156.
6. Ezan J, et al. (2013) Primary cilium migration depends on G-protein signalling control of subapical cytoskeleton. *Nat Cell Biol* 15:1107–1115.
7. Tarchini B, Jolicoeur C, Cayouette M (2013) A molecular blueprint at the apical surface establishes planar asymmetry in cochlear hair cells. *Dev Cell* 27:88–102.
8. Bhonker Y, et al. (2016) The GPSM2/LGN GoLoco motifs are essential for hearing. *Mamm Genome* 27:29–46.
9. Forge A, Taylor RR, Dawson SJ, Lovett M, Jagger DJ (2017) Disruption of SorCS2 reveals differences in the regulation of stereociliary bundle formation between hair cell types in the inner ear. *PLoS Genet* 13:e1006692.
10. May-Simera HL, et al. (2015) Ciliary proteins Bbs8 and Ift20 promote planar cell polarity in the cochlea. *Development* 142:555–566.
11. Ishida-Takagishi M, et al. (2012) The Dishevelled-associating protein Daple controls the non-canonical Wnt/Rac pathway and cell motility. *Nat Commun* 3:859.
12. Ara H, et al. (2016) Role for Daple in non-canonical Wnt signaling during gastric cancer invasion and metastasis. *Cancer Sci* 107:133–139.
13. Aznar N, et al. (2015) Daple is a novel non-receptor GEF required for trimeric G protein activation in Wnt signaling. *Elife* 4:e07091.
14. Oshita A, et al. (2003) Identification and characterization of a novel Dvl-binding protein that suppresses Wnt signalling pathway. *Genes Cells* 8:1005–1017.
15. Kobayashi H, et al. (2005) Novel Daple-like protein positively regulates both the Wnt/beta-catenin pathway and the Wnt/JNK pathway in Xenopus. *Mech Dev* 122: 1138–1153.
16. Wang J, et al. (2005) Regulation of polarized extension and planar cell polarity in the cochlea by the vertebrate PCP pathway. *Nat Genet* 37:980–985.
17. Wang J, et al. (2006) Dishevelled genes mediate a conserved mammalian PCP pathway to regulate convergent extension during neurulation. *Development* 133: 1767–1778.
18. Etheridge SL, et al. (2008) Murine dishevelled 3 functions in redundant pathways with dishevelled 1 and 2 in normal cardiac outflow tract, cochlea, and neural tube development. *PLoS Genet* 4:e1000259.
19. Montcouquiol M, et al. (2006) Asymmetric localization of Vangl2 and Fz3 indicate novel mechanisms for planar cell polarity in mammals. *J Neurosci* 26:5265–5275.
20. Copley CO, Duncan JS, Liu C, Cheng H, Deans MR (2013) Postnatal refinement of auditory hair cell planar polarity deficits occurs in the absence of Vangl2. *J Neurosci* 33:14001–14016.
21. Zheng JL, Gao WQ (2000) Overexpression of Math1 induces robust production of extra hair cells in postnatal rat inner ears. *Nat Neurosci* 3:580–586.
22. Jiang T, Kindt K, Wu DK (2017) Transcription factor Emx2 controls stereociliary bundle orientation of sensory hair cells. *Elife* 6:e23661.
23. Hébert JM, McConnell SK (2000) Targeting of cre to the Foxg1 (BF-1) locus mediates loxP recombination in the telencephalon and other developing head structures. *Dev Biol* 222:296–306.
24. Tarchini B, Tadenev AL, Devanney N, Cayouette M (2016) A link between planar polarity and staircase-like bundle architecture in hair cells. *Development* 143:3926–3931.
25. Cho H, Kim DU, Kehrl JH (2005) RGS14 is a centrosomal and nuclear cytoplasmic shuttling protein that traffics to promyelocytic leukemia nuclear bodies following heat shock. *J Biol Chem* 280:805–814.
26. Cho H, Kehrl JH (2007) Localization of Gi alpha proteins in the centrosomes and at the midbody: Implication for their role in cell division. *J Cell Biol* 178:245–255.
27. Williams SE, Beronja S, Pasolli HA, Fuchs E (2011) Asymmetric cell divisions promote Notch-dependent epidermal differentiation. *Nature* 470:353–358.
28. Ségalen M, et al. (2010) The Fz-Dsh planar cell polarity pathway induces oriented cell division via Mud/NuMA in Drosophila and zebrafish. *Dev Cell* 19:740–752.
29. Takagishi M, et al. (2017) Daple coordinates planar polarized microtubule dynamics in ependymal cells and contributes to hydrocephalus. *Cell Rep* 20:960–972.